Weak lensing evidence for a filament between A222/A223*

J. P. Dietrich†, D. Clowe, P. Schneider
IAEF, University of Bonn
J. Kerp
Radioastronomisches Institut, University of Bonn
E. Romano-Díaz
Kapteyn Institute, University of Groningen

Abstract

We present a weak lensing analysis and comparison to optical and X-ray maps of the close pair of massive clusters A222/223. Indications for a filamentary connection between the clusters are found and discussed.

1 Introduction

N-body simulations of cosmic structure formation predicts that matter in the universe should be concentrated along sheets and filaments and that clusters of galaxies form where these intersect (Kauffmann et al. 1999; Bond et al. 1996). This filamentary structure, often also dubbed "cosmic web", has been seen in galaxy redshift surveys (Vogeley et al. 1994) and X-rays (Zappacosta et al. 2002; Tittley & Henriksen 2001).

Because of the greatly varying mass–to–light (M/L) ratios between rich clusters and groups of galaxies (Tully & Shaya 1998) it is problematic to convert the measured galaxy densities to mass densities without further assumptions. Weak gravitational lensing, which is based on the measurement of shape and orientation parameters of faint background galaxies (FBG), is a model–independent method to determine the surface mass density of clusters and filaments. Due to the finite ellipticities of the unlensed FBG, every weak lensing mass reconstruction is unfortunately an inherently noisy process, and the expected surface mass density of a single filament is too low to be detected with current telescopes (Jain et al. 2000).

*Based on observations made at ESO/La Silla under program Nos. 064.L-0248, 064.O-0248, 66.A-0165, 68.A-0269.

†dietrich@astro.uni-bonn.de

Cosmic web theory also predicts that the surface mass density of a filament increases towards clusters (Bond et al. 1996). Filaments connecting neighboring clusters should have surface mass densities high enough to be detectable with weak lensing (Pogosyan et al. 1998). Such filaments may have been detected in several recent weak lensing studies.

Kaiser et al. (1998) found a possible filament between two of the three clusters in the $z = 0.42$ super-cluster MS0302+17, but the detection remains somewhat uncertain because of a possible foreground structure overlapping the filament and possible edge effects due to the gap between two of the camera chips lying along the filament. Also, Gavazzi et al. (2004) could not confirm the detection of a filament in this system. Gray et al. (2002) claim to have found a filament extending between two of the three clusters of the Abell 901/902 super-cluster, but the significance of this detection is low and subject to possible edge effects, as again the filament is close the intersection of four chips of the camera.

2 Data of the Abell 222/223 system

A 222/223 are two Abell clusters at $z \approx 0.21$ separated by $\sim 14'$ on the sky, or $\sim 2600 h_{70}^{-1}$ kpc, belonging to the Butcher et al. (1983) photometric sample. Both clusters are rich, having Abell richness class 3 (Abell 1958). While these are optically selected clusters, they have been observed by ROSAT (Wang & Ulmer 1997; David et al. 1999) and are confirmed to be massive clusters. Proust et al. (2000, P00) published a list of 53 spectra in the field of A 222/223, 4 of them in region between the clusters (hereafter "intercluster region") and at the redshift of the clusters. Later, Dietrich et al. (2002, D02) reported on spectroscopy of 183 objects in the cluster field, 153 being members of the clusters or at the cluster redshift in the intercluster region. Taking the data of P00 and D02 together, 6 galaxies at the cluster redshift are known in the intercluster region, establishing this cluster system as a good candidate for a filamentary connection.

Imaging was performed with the Wide Field Imager (WFI) at the ESO/MPG 2.2 m telescope. In total, twenty 600 s exposures were obtained in R-band in October 2001 centered on A223, eleven 900 s R-band exposures were taken in December 1999 centered on A 222. The images were taken with a dithering pattern filling the gaps between the chips in the co-added images of each field.

The R-band data used for the weak lensing analysis is supplemented with three 900 s in the B and V-band centered on each cluster taken from November 1999 to December 2000. The final B- and V-band images have some remaining gaps and regions that are covered by only one exposure and – due to the dithering pattern – do not cover exactly the same region as the R-band images.

2.1 Catalog creation

Lensing catalogs were created from the R-band images using the KSB algorithm (Kaiser et al. 1995). Stellar reflection rings and diffraction spikes were masked

and the masked regions excluded from the catalogs. The catalogs from both pointings were merged and the ellipticities of objects contained in both catalogs were averaged.

From this merged catalog all objects with $R < 22$ mag, signal-to-noise $\nu < 7$, Gaussian radius $0\farcs4 < r_{\rm g} < 1\farcs2$, and ellipticity $e > 0.8$ were deleted. All surviving objects fainter than $R > 23.5$ mag were kept as likely background galaxies, while objects brighter than this – for which colors were available – were selected according to the following criteria: Objects detected in B, V, and R matching colors of galaxies at $z < 0.5$, $-0.23 < (V - R) - 0.56 \times (B - V) < 0.67$, $0.5 < B - V < 1.6$, were deleted from the sample. Galaxies detected only in the V and R band were kept if $(V - R) > 1.0$. The final catalog contains 25583 objects, corresponding to a galaxy number density of 15.5 arcmin^{-2} if the masked regions are not taken into account for the computation of the total area.

3 Mass and light maps

Fig. 1 shows a reconstruction obtained from the catalog described in the previous section. The reconstruction was performed on a 214×200 points grid using the algorithm of Seitz & Schneider (2001) adapted to the field geometry. The smoothing scale of the shear data was set to $2'$. Galaxies in the catalog were weighted by the error estimate of their initial ellipticity measurement.

Both clusters are well detected in the reconstruction. The two components of A 223 are clearly visible. The strong mass peak West of A 223 is most likely associated with the reflection ring around the bright $V = 7.98$ mag star at that position. Although the reflection ring and a large area around it were masked, diffuse stray light is visible extending beyond the masked region, well into A 223, probably being the cause of the observed mass peak.

Also visible is a bridge in the surface mass density extending between A 222 and A 223. Although the signal of this possible filamentary connection between the clusters is very low, the feature is quite robust when the selection criteria of the catalog are varied and it never disappears.

The noise level in the reconstruction can be estimated by randomly rotating the galaxies while keeping their positions and ellipticity moduli fixed. Performing a reconstruction on this randomized catalog gives $\langle \kappa^2 \rangle \simeq 0.015$, suggesting that the intercluster connection is present at the $\sim 2\sigma$ level.

The galaxy density distribution and the X-ray contours in Fig. 1 both show a clear connection between the clusters. While the X-ray and galaxy density contours are aligned in the intercluster region, the surface mass density contours connect the clusters Eastwards of them.

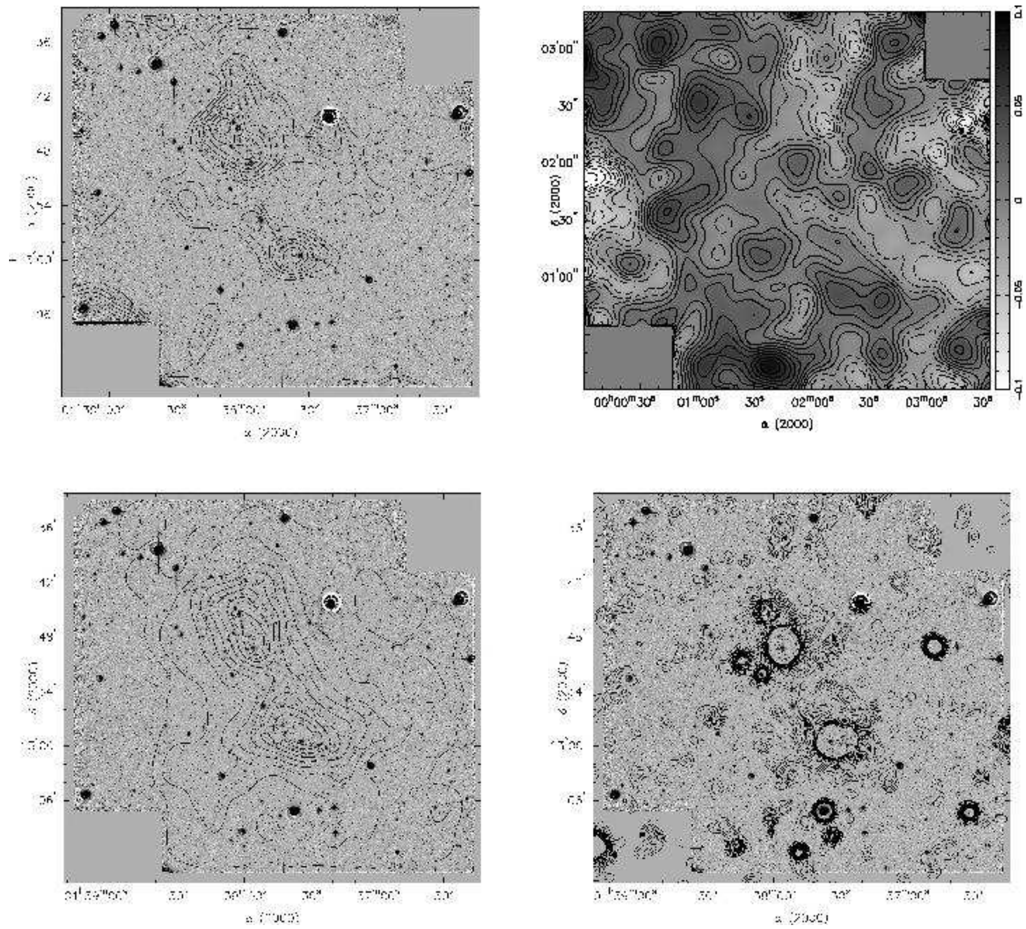

Figure 1: Various light and mass maps of the A 222/223 system. A 223 is the Northern cluster, A 222 is South of it. *Top left*: Weak lensing reconstruction of A222/223. Each contour represents an increase in κ of 0.01 ($\sim 3.2 \times 10^{13}\ h_{70}\ M_{\odot}\ \mathrm{Mpc}^{-2}$, assuming $\overline{z}_{\mathrm{FBG}} = 1$) above the mean κ at the edge of the field. The peak $\sim 12'$ SE of A 222 has an optical counter-part. *Top right*: Surface mass density map created from a catalog with randomly rotated galaxies used to estimate the noise level of the reconstruction on the right. *Bottom left*: Density distribution of galaxies matching the colors of the red cluster sequence ($0.78 < V - R < 0.98$) of the Abell clusters smoothed with a $2'$ Gaussian. The absence of galaxies in the Eastern part is caused by the very bad or missing V-band coverage. *Bottom right*: Contours in this plot are from ROSAT PSPC data in the energy range $0.5 - 2.4$ keV. The lowest contour is at the 6σ level. Higher contours rise in steps of 1σ. Note that the extended X-ray emission North of A 223 is associated with the Northern extension of A 223 in the surface mass density map.

4 Discussion

We presented weak lensing, optical galaxy density, and X-ray maps of the massive, close pair of galaxy clusters A 222/223. All maps show a connection between the clusters in the intercluster region. The density distribution of color-selected objects, supplemented by the spectroscopic confirmation of galaxies at the cluster redshift in the intercluster region by P00 and D02, and the significant connection between both clusters in the $0.5 - 2.4$ keV band of ROSAT's PSPC establish a secure filamentary connection between the clusters. The weak lensing indications for a dark matter bridge are much less secure. The signal-to-noise of the structure extending between the clusters is low but the structure itself is very robust and never disappears when the selection criteria for the lensing catalog are varied.

We note that the luminosity density of color-selected galaxies in the intercluster region is only by a factor of ~ 2 lower than in the peaks of the galaxy clusters. If the early type galaxies trace the mass well and a constant M/L ratio is assumed, we would expect a clearly detectable lensing signal along the galaxy density contours. This is obviously not the case. A more detailled comparison of the observed and expected surface mass density, also addressing the apparent misalignment of mass and light in A 223, will be done elsewhere (Dietrich et al. 2004, in preparation). We also note that a misalignment of mass and light is present in the filament candidate of Gray et al. (2002).

Acknowledgment: This work has been supported by the German Ministry for Science and Education (BMBF) through DESY under the project 05AE2PDA/8, and by the Deutsche Forschungsgemeinschaft under the project SCHN 342/3–1.

References

Abell, G. O. 1958, ApJS, 3, 211

Bond, H., Kofman, L., & Pogosyan, D. 1996, Nature, 380, 603

Bruzual, A. G. & Charlot, S. 1993, ApJ, 405, 538

Butcher, H., Wells, D. C., & Oemler, A. 1983, ApJS, 52, 183

David, L. P., Forman, W., & Jones, C. 1999, ApJ, 519, 533

Dietrich, J. P., Clowe, D. I., & Soucail, G. 2002, A&A, 394, 395

Gavazzi, R., Mellier, Y., Fort, B., Cuillandre, J. ., & Dantel-Fort, M. 2004, astro-ph/0401403

Gray, M. E., Taylor, A. N., Meisenheimer, K., et al. 2002, ApJ, 568, 141

Jain, B., Seljak, U., & White, S. 2000, ApJ, 530, 547

Kaiser, N., Squires, G., & Broadhurst, T. 1995, ApJ, 449, 460

Kaiser, N., Wilson, G., Luppino, G., et al. 1998, astro-ph/99809268

Kauffmann, G., Colberg, J. M., Diaferio, A., & White, S. D. M. 1999, MNRAS, 303, 188

Pogosyan, D., Bond, J. R., Kofman, L., & Wadsley, J. 1998, in Wide Field Surveys in Cosmology, 14th IAP meeting held May 26-30, 1998, Paris. Publisher: Editions Frontieres. ISBN: 2-8 6332-241-9, 61

Proust, D., Cuevas, H., Capelato, H. V., et al. 2000, A&A, 355, 443

Schirmer, M., Erben, T., Schneider, P., et al. 2003, A&A, 407, 869

Schlegel, D. J., Finkbeiner, D. P., & Davis, M. 1998, ApJ, 500, 525

Seitz, S. & Schneider, P. 2001, A&A, 374, 740

Tittley, E. R. & Henriksen, M. 2001, ApJ, 563, 673

Tully, R. B. & Shaya, E. J. 1998, astro-ph/9810298

Vogeley, M. S., Park, C., Geller, M. J., Huchra, J. P., & Gott, J. R. I. 1994, ApJ, 420, 525

Wang, Q. D. & Ulmer, M. P. 1997, MNRAS, 292, 920

Zappacosta, L., Mannucci, F., Maiolino, R., et al. 2002, A&A, 394, 7